Cytosine-rich DNA Binding Insulin Stronger than Guanine-rich Aptamers: Effect of Aggregation of Insulin for Its Detection

Na Wu[a, b], Mohamad Zandieh[b], Ting Yang[a] and Juewen Liu[b*]

[a] Research Center for Analytical Sciences, Department of Chemistry, College of Sciences, Northeastern University, Box 332, Shenyang 110819, China

[b] Department of Chemistry, Waterloo Institute for Nanotechnology, University of Waterloo, Waterloo, Ontario N2L 3G1, Canada

Email: liujw@uwaterloo.ca

ABSTRACT

The detection of insulin is an important analytical task. Previously, guanine-rich DNA was believed to bind insulin and an insulin aptamer was selected based on a few guanine-rich libraries. Insulin is a unique analyte and it forms different aggregation states as a function of its concentration and buffer conditions, which may affect the detection of insulin. Herein using fluorescence polarization assays, three insulin preparation methods were evaluated: direct dissolution, EDTA treatment to remove Zn^{2+}, and dissolution in acid followed by neutralization. All the insulin samples containing Zn^{2+} barely bind to the aptamer DNA, whereas monomers and dimers of insulin with Zn^{2+} removed were able to bind. Compared to the previously reported aptamer, C-rich DNA showed stronger binding affinities and faster binding kinetics. Based on the sigmoidal binding curves and slow binding kinetics, multiple DNA strands and insulin molecules gradually bind, and it took approximately 1 h to reach saturation. This binding was non-specific and other tested proteins also can bind to C-rich and G-rich DNA with even strong affinities. These results provide important information on the detection of insulin and further insights into the binding mechanisms between oligomeric insulin and DNA.

INTRODUCTION

Insulin is a short peptide hormone essential for the regulation of glucose metabolism.[1] It is made up of two peptide chains joined by two disulfide bonds.[2] Depending on its concentration, pH, salt type and salt concentration, insulin exits in an equilibrium of monomers, dimers, tetramers, hexamers, and even higher aggregated states.[3-5] The predominant physiological storage form of insulin is a hexamer, in which two to four Zn^{2+} ions associate three dimer units.[6-8] In the absence of Zn^{2+}, insulin is a dimer at low concentrations but becomes a tetramer at >1.5 mg/mL.[9-10]

In 1996, Gupta et al. found a DNA sequence 363 base pair (bp) upstream of the human insulin gene that contains many consecutive G-rich sequences (called the insulin-linked polymorphic repeat region or ILPR), suggesting that a G-quadruplex structure might be involved in the expression of the human insulin gene.[11] Owing to the polymorphic character of the G-rich region of ILPR, 14 different variants (repeats *a* to *n*) have been identified.[12] The repeats *a* (ACAG4TGTG4), *b* (ACAG4TCTG4) and *c* (ACAG4TCCTG4) are the most common accounting for 80% of the known sequences in the total ILPR.[13] McGown et al. reported that human insulin exhibited an affinity to an ILPR variant (ACAG4TGTG4ACAG4TGTG4) in vitro.[14] This finding intrigued other researchers regarding whether insulin can bind to other types of G-quadruplexes. Ikebukuro and coworkers designed six aptamer selection libraries all based on G-quadruplex DNA.[15] They selected the IGA3 aptamer (GGTGGTG8TTGGTAG3TGTCTTC), which exhibited a higher binding affinity to insulin. This aptamer has been used to develop biosensors for the detection of insulin.[16-20]

Insulin exists in distinct aggregation forms under different conditions, which would affect the physiological functions of insulin.[21-24] In addition, different aggregated forms may also bind differently to aptamers. While binding studies were previously reported for the insulin aptamer,[25-26] none of them was explicit about the aggregation forms of insulin. To address this important problem, we herein studied insulin samples prepared under different conditions corresponding to different aggregation states by adjusting pH and EDTA concentrations. In addition to the G-rich IGA3 aptamer, we also studied a few other DNA sequences. Surprisingly, we found much stronger insulin binding with cytosine (C)-rich DNA. Insights regarding the biosensing of insulin have been gained by studying the kinetics of insulin binding.

MATERIALS AND METHODS

Materials

All of the DNA samples were purchased from Integrated DNA Technologies (Coralville, IA, USA; see Table S1 for sequences). Recombinant Insulin human in powder form was from Sigma-Aldrich (catalog number: 91077C, manufactured by SAFC Biosciences Inc., Lenexa. KS. USA). 8-Hydroxy-5-quinolinesulfonic acid (HQS), fluorescein, thioflavin T (ThT), bovine serum albumin (BSA), hemoglobin, and human albumin were obtained from Sigma-Aldrich. Milli-Q water was used to prepare all the solutions and buffers.

Preparation of Insulin Samples

Recombinant human insulin (0.6 mg) was weighed and dissolved into 1 mL of buffer (in 25 mM Tris-HCl pH 7.4, 10 mM KCl, 100 mM NaCl) to a concentration of 100 μM. To prepare insulin fibrils, 100 μM insulin was added to 0.04 M hydrochloric acid (pH 1.6) and 0.1 M NaCl and subsequently stored at 4 °C for 48 h.

Dynamic Light Scattering (DLS) Characterization

The size and size distribution of insulin (hexamer, dimer, and monomer) in the buffer (25 mM Tris-HCl pH 7.4, 10 mM KCl, and 100 mM NaCl) were measured using a Nano Zetasizer system (Malvern Instruments). Insulin (50 μM) was loaded into a quartz microcuvette and five measurements were performed for each sample.

Transmission Electronic Microscopy (TEM) Characterization

The solution (10 μM of Zn^{2+}-insulin and 50 μM of Zn^{2+}-insulin) was spotted on a copper TEM grid. After 10 min, 2% freshly prepared phosphotungstic acid was added dropwise for staining. Dried samples were observed under a TEM microscope (Philips CM10, USA) operated at an accelerating voltage of 60 kV.

Thioflavin T Fluorescence Assays for Insulin Amyloid Fibrils

ThT (10 mM in anhydrous alcohol) was prepared and stored at 4°C in dark. For ThT fluorescence spectroscopy, a final of 2 μM ThT was added in a 96-microwell microplate with 100 μL insulin.

The samples were measured in a Tecan Spark plate reader at room temperature (excitation at 444 nm, emission at 485 nm).

Binding Assay of Insulin to DNA

FAM-labeled aptamer DNA (100 nM) was heated to 95℃ for 5 min and gradually cooled in Tris-HCl buffer (25 mM Tris-HCl, pH 8.0, 10 mM KCl, 100 mM NaCl). Insulin was diluted freshly before each experiment to a concentration of 100 μM in 25 mM Tris-HCl pH 7.4, 10 mM KCl, 100 mM NaCl. The above insulin (25 μM) was incubated with a final of 12 mM of EDTA for 15 min in an ice bath. Then, FAM-aptamer or other DNA was incubated with various concentration of insulin (treated with EDTA) for 60 min. The FP of the FAM-labeled aptamer was measured by the Tecan fluorescence plate reader at 485 nm excitation and 530 nm emission at room temperature.

Cy3-Labeled DNA at Different pH

The Cy3-C15 DNA (40 nM) was mixed with insulin (Zn^{2+}-free and Zn^{2+}) (25 μM), and the pH was adjusted to 5.0 (20 mM citrate buffer), 6.0 (20 mM MES buffer), 7.4 (25 mM Tirs-HCl buffer) and 8.2 (25 mM Tris-HCl buffer), respectively for 60 min at 37 ℃. The FP of the Cy3-labeled C15 DNA was measured by the Tecan fluorescence plate reader at 545 nm excitation and 572 nm emission at room temperature.

Data Fitting.

The Finke-Watzky (F-W) two-step model of nucleation and followed autocatalytic growth was used to fitting the time-dependent fluorescence polarization plots obtained from the Zn-free insulin binding DNA (IGA3 aptamer and i-motif) experiments.[27] All kinetic data were processed by Origin Pro 2019.

RESULTS AND DISCUSSION

Aggregation States of Insulin

An insulin molecule is consists of two peptide chains (21 and 30 amino acids) crosslinked by two disulfide bridges (Figure 1A).[28] Insulin can easily aggregate to form aggregates or fibrils depending on buffer conditions.[29] For example, Zn^{2+} promotes the hexamer form, while Zn^{2+}-free

insulin often exists in dimers (Figure 1B).[9] Oligomeric insulin structures (tetramer, dimers, and monomers) have low stability.[30-31] We were interested in understanding the effect of aptamer binding on different aggregation states of insulin.

The insulin samples used in this study contained Zn^{2+}. When freshly dissolved in water at 100 μM, insulin appeared as a cloudy suspension (Figure 1C), indicating strong aggregation. To reduce aggregation, we added 12 mM EDTA to chelate Zn^{2+}, which made a solution clear (Figure 1C). To test whether the cloudy suspension was due to fibrils, we added thioflavin T (ThT) to stain amyloids,[32] which should enhance ThT emission at 482 nm.[33] The freshly prepared insulin (50 μM) did not show any fluorescence change at pH 7.4 (Figure 1D). However, when we stored insulin in 25 mM HCl (pH 1.6) for 2 days and added ThT to this sample, a fluorescence increase was observed, which was consistent with fibril formation at low pH.[33] Thus, the freshly prepared insulin sample was in an aggregated state, but the aggregates were not fibrils. In addition, freshly prepared Zn^{2+}-free insulin did not show any fluorescence changes (Figure S1). Therefore, under normal experimental conditions of less than 50 μM insulin (with Zn^{2+} or Zn^{2+}-free) and pH 7.4, we do not need to consider the fiber formation.

We also characterized the aggregation state of insulin by DLS (Figure 1E). Freshly prepared insulin had a strong scattering peak above 1 μm, consistent with the visually observable large aggregates. After treatment with EDTA, the main peak shifted below 10 nm, although a peak at ~500 nm was observed. Because this is a plot of scattering intensity, the population at 500 nm is an insignificant portion of the EDTA-added sample. The morphology of insulin aggregates in the presence or absence of Zn^{2+} was observed by transmission electronic microscopy (TEM). TEM confirmed a large number of aggregates for the Zn^{2+}-insulin. (Figure S2A). In the Zn^{2+}-free insulin, small and dispersed aggregates were identified consistent with the DLS data (Figure S2B). Therefore, insulin mainly existed in aggregated oligomers without EDTA, and EDTA can break such aggregates.

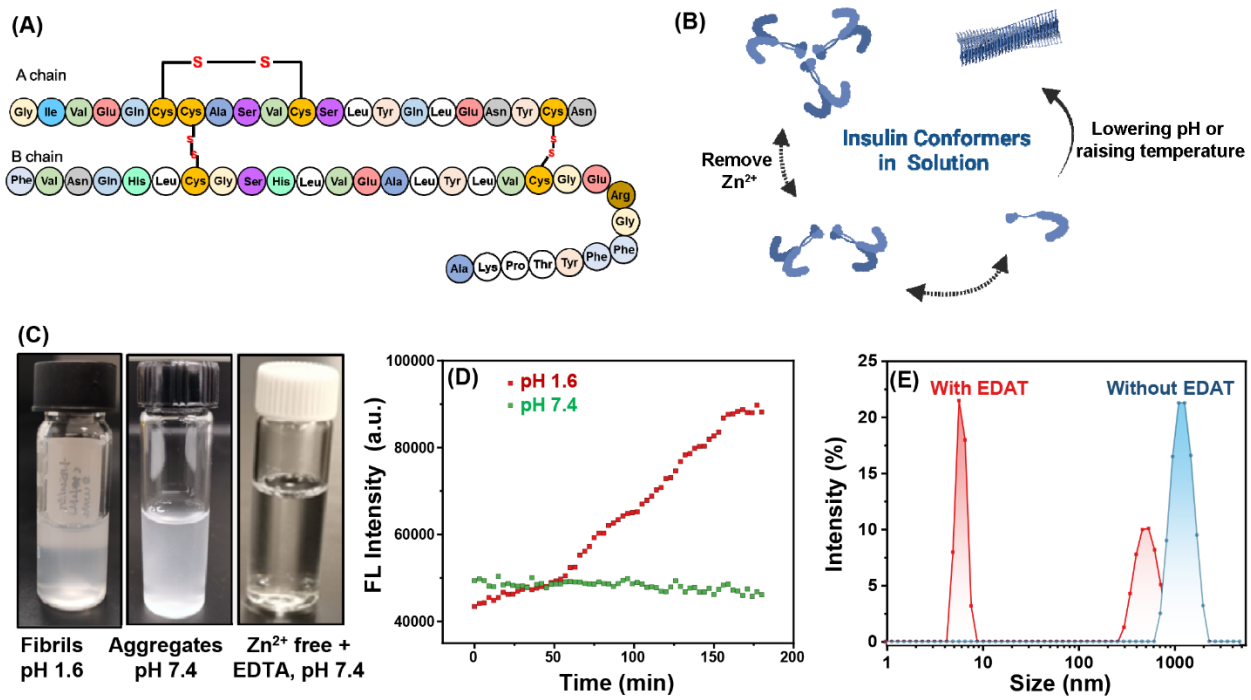


Figure 1. (A) The amino acid sequence of human insulin. (B) The conversion of various aggregation forms of insulin in solution. (C) Photographs of insulin fibril prepared at pH 1.6, Zn^{2+}-insulin prepared by directly dissolving insulin in a neutral pH buffer, and Zn^{2+}-free insulin prepared by adding EDTA. The insulin concentration in the photos was 100 μM. (D) Kinetics of ThT fluorescence for staining insulin fibrils. The insulin concentration was 50 μM dissolved in 25 mM HCl and 0.1 M NaCl (pH 1.6) or in pH 7.4 buffer. (E) The DLS of 50 μM insulin (Zn^{2+}-insulin: blue line) and 50 μM insulin (Zn^{2+}-free insulin: red line).

Zn^{2+}-free Insulin Binding to G-Quadruplex DNA

To study aptamer binding, we first used the IGA3 aptamer, whose G-quadruplex loop region was proposed to be a potential insulin binding site.[16] Since the aggregation state of insulin might influence aptamer binding, we prepared insulin using three methods: (1) direct dissolution in the neutral pH buffer resulting in aggregates; (2) dissolution in 5 mM HCl for 10 min (before fibril formation) and then adjustment to neutral pH, resulting in a clear solution; and (3) with 12 mM EDTA, resulting in a clear solution (Figure 2B). Using HQS as a Zn^{2+} probe, the Zn^{2+} concentration in 100 μM insulin was measured to be 16 μM (Figure S3). Therefore, 12 mM EDTA was in great excess.

To monitor aptamer binding, the IAG3 aptamer was labeled with a FAM fluorophore to perform a fluorescence polarization (FP) assay. Upon insulin binding, an increase in FP was expected. As a control, we first investigated the effect of free fluorescein fluorophore to insulin. As shown in Figure S4, no change in the FP signal was observed with increasing insulin concentration indicating that the fluorophore does not bind to insulin. We then used two aptamer concentrations, 100 nM and 10 nM. As shown in Figure 2B, Zn^{2+}-containing insulin (prepared using methods 1 and 2) showed no signs of binding with up to 60 μM insulin. In contrast, for the EDTA-added sample (Zn^{2+} free), an increased FP was observed when the insulin concentration was higher than 20 μM, and the FP increased with increasing insulin concentration. Since more than 20 μM insulin was required to show obvious binding, multiple insulin molecules were needed to achieve a cooperative effect, suggesting that the aptamer was bound to an aggregated insulin form. However, this aggregated form differed from the aggregates formed in the presence of Zn^{2+}, which did not bind to the IAG3 aptamer. This sigmoidal binding curve is consistent with the literature, where the sequence of the IAG3 aptamer was first reported.[16] Although in that paper, the method of preparing insulin samples was not explicitly reported, we suspected that the authors might have used a similar EDTA treatment or directly used Zn^{2+}-free insulin.

Of the two aptamer concentrations tested, a less obvious signal change was observed with the 10 nM aptamer sample (Figure 2C), suggesting that the binding might also involve multiple aptamer strands. Otherwise, the FP measurements should be independent of the aptamer concentration.

The capability of EDTA to chelate Zn^{2+} determines whether insulin is present as a hexamer or an oligomer under neutral buffer conditions.[24-25] We then studied the effect of EDTA concentration. The FP signal increased as the EDTA concentration increased (Figure S5), and a plateau was observed at EDTA concentrations higher than 12 mM. Considering the low concentration of Zn^{2+} in the system, the need for very high EDTA concentrations suggests that insulin has a strong affinity for Zn^{2+}. The insulin aggregation states are significantly influenced by ionic strength, [34] which may also impact insulin binding to DNA. Therefore, we measured binding with different concentrations of Na^{+} and Mg^{2+} by incubating with 25 μM insulin for 30 min, followed by the introduction of 100 nM of the aptamer. As shown in Figure S6, in the Zn^{2+}-free insulin sample, the binding became less obvious with increasing ionic strength, suggesting that a high salt concentration can inhibit aptamer binding.

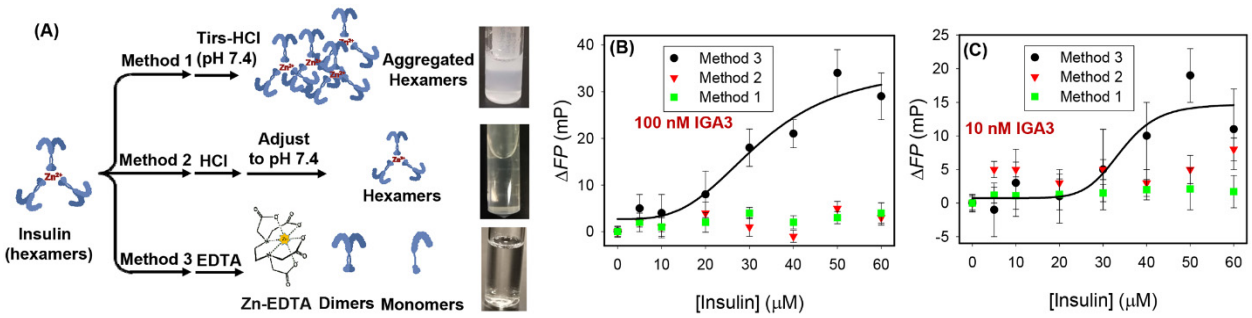


Figure 2. (A) Three types of insulin treatment. Method 1: insulin dissolved in pH 7.4 Tris-HCl buffer. Method 2: insulin dissolved in 5 mM HCl then adjusted to neutral pH. Method 3: insulin dissolved in 12 mM EDTA. The binding of insulin treated with different methods to (B) 100 nM and (C) 10 nM of the IGA3 aptamer.

Cytosine-rich DNA with Even Better Binding to Insulin.

All previous studies have focused on the G-rich DNA aptamer due to the DNA sequences upstream of the insulin gene.[11-14] However, this is not a strong support that insulin aptamers have to be G-rich DNA sequences. Since the tested aptamer showed atypical binding (aptamer concentration dependency and lack of binding at low insulin concentrations), we further explored the effect of other DNA sequences as controls. FAM-labeled poly-A and poly-T DNA did not show a change in FP value, whereas most C- and G-rich DNA showed increased FP upon adding insulin (Figure 3A). It might be that the oligomeric state of insulin can interact with guanine and cytosine bases in DNA.[35]

Interestingly, the increase in FP of poly-C was higher than that of poly-G, and longer poly-C DNA showed a larger increase (Figure 3A). In light of Zn^{2+}-free insulin binding to G-rich and C-rich DNA, the complementary sequence of the IGA3 aptamer (named cIGA3) was also tested. As shown in Figure 3B, FAM-cIGA3 could also bind to Zn^{2+}-free insulin with a large FP increase, whereas Zn^{2+}-containing insulin showed no binding. The increase in FP was also greater with higher concentrations of FAM-cIGA3, also suggesting that more than one DNA might be involved in the formation of the binding complex.

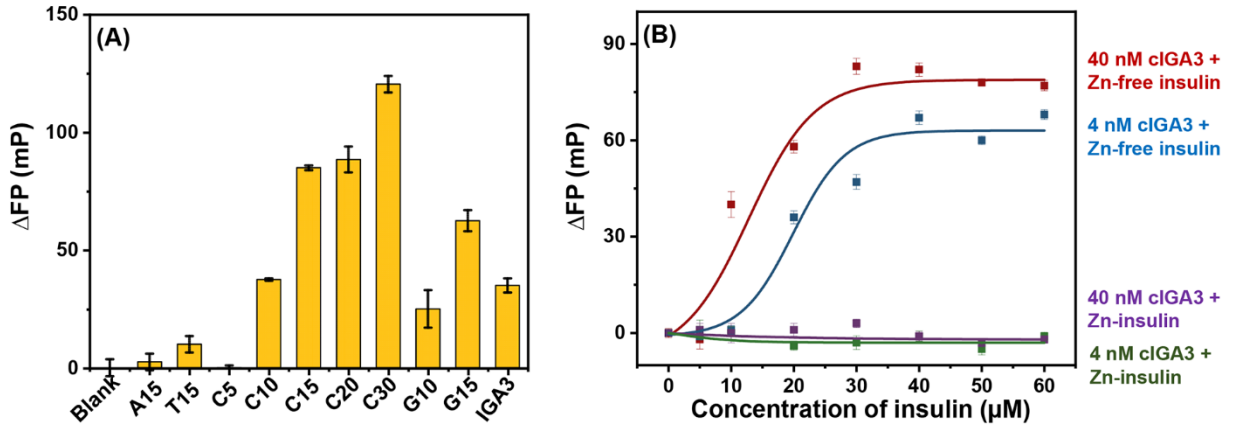


Figure 3. (A) The Zn^{2+}-free insulin (25 μM) binding by various FAM-labeled DNA (100 nM). (B) FP change of the FAM-cIGA3 DNA as a function of insulin concentration for the Zn^{2+}-free insulin prepared using method 3 and Zn^{2+}-containing insulin prepared with method 1.

To further elucidate the binding between insulin and poly-C DNA, FP titration curves of three different C-rich DNA (C_{20}, C_{30}, and cIGA3) were collected (Figure 4). The binding curves were fitted with the Hill equation,[36] and the Hill coefficients were determined for C_{20} (3.8), C_{30} (2.7), and the cIGA3 (2.8), suggesting that all these DNAs bind insulin in a cooperative manner. In other words, three to four insulin molecules bind to the DNAs, and binding of the next insulin molecules was facilitated by the binding of the previous ones. In this regard, the C-rich DNAs and the IGA3 aptamer were similar. In contrast, the onset of binding appeared at lower insulin concentrations for the C-rich DNA. For example, cIGA3 showed binding even with 6 μM insulin (Figure 4C), whereas IGA3 showed binding with 20 μM insulin (Figure 2B).

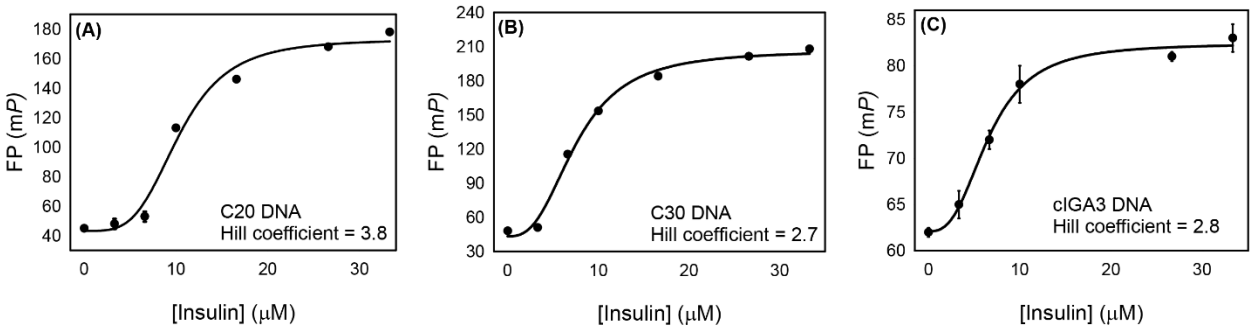


Figure 4. (A) Different concentration of insulin binding to FAM-labeled (A) C20, (B) C30, and (C) cIGA3 DNA monitored using FP. The binding curves were fitted using the Hill equation.

Slow Binding Kinetics Indicative of DNA-Induced Insulin Aggregation. Since the binding involved multiple insulin molecules and DNA strands, we studied the kinetics of insulin binding. Upon mixing the EDTA-treated Zn^{2+}-free insulin with the IGA3 aptamer, FP gradually increased and became saturated after 80 min. As expected, the signal of the Zn^{2+}-containing samples hardly changed (prepared using method 1, Figure 5A). To understand the reason for the slow kinetics, insulin was mixed with EDTA and incubated for different periods before adding the IAG3 aptamer, and these samples showed no significant difference (Figure S7). This result suggested that Zn^{2+}-free insulin in the presence of excess EDTA did not undergo significant aggregation over a day, and the slow kinetics we observed was due to DNA binding.

We then compared the kinetics of IGA3 with cIGA3 (Figure 5B). Interestingly, the cIGA3 DNA showed faster initial binding kinetics, although it still took approximately 1 h for binding to reach saturation. The shape of the kinetic traces was similar from that of the G-rich IGA3 aptamer, and we observe the initial induction period with cIGA3. The binding kinetics for cIGA3 (C-rich) were fitted using Finke-Watzky (F-W) two-step model (Figure 5B), and the rate constants were κ=0.024 min^{-1} and κ=0.033 min^{-1} for 4 nM and 40 nM cIGA3 DNA, respectively. The F-W two-step model of nucleation followed by autocatalytic growth provides an analytical description of our kinetic data.[27]

The slow kinetics observed was attributed to insulin aggregation on the DNA. This is also consistent with the above insulin concentration-dependent study, indicating that multiple insulins are associated with DNA. After losing Zn^{2+}, insulin monomers and dimers use negatively charged DNA as a nuclear aggregate, which in turn increases the FP of the FAM-labeled DNA. In the presence of C-rich or G-rich DNA, insulin monomers and dimers gradually bind to it. The initial binding was weak and stable binding was achieved only when a few insulin molecules were bound to multiple DNA strands.

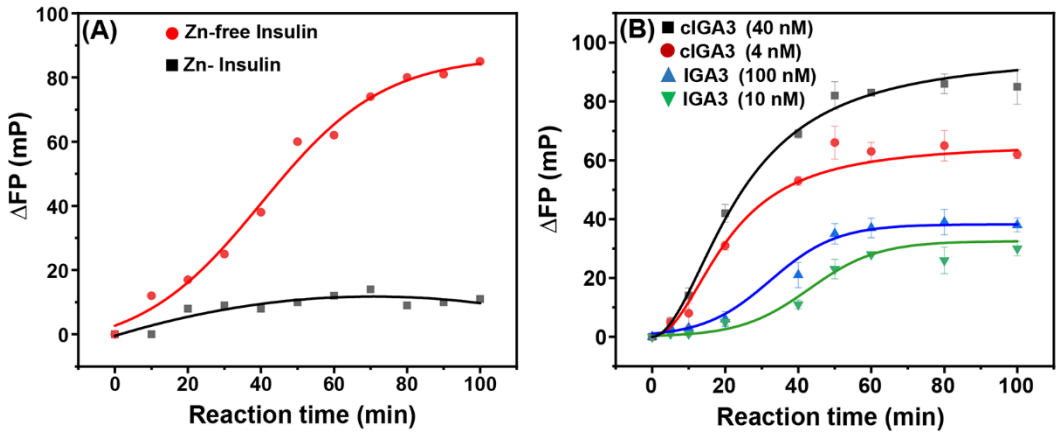


Figure 5. (A) The kinetics of insulin (25 μM) binding to the IGA3 aptamer (100 nM) over time for the two types of insulin samples. (B) The kinetic profile of Zn^{2+}-free insulin binding to cIGA3 (40 nM and 4 nM) and the IGA3 aptamer (100 nM and 10 nM).

Poly-C DNA Binding Insulin Better at Higher pH.

Poly-C DNA and also the cIGA3 sequence may form i-motif structures. To test whether insulin binding was related to i-motif formation, we measured pH-dependent insulin binding since i-motif is promoted at acidic pH. The change in FP of Cy3-modified C15 DNA was monitored by adding Zn^{2+}-containing and Zn^{2+}-free insulin from pH 5.0 to 8.2 (Figure 6A). Zn^{2+}-free insulin showed weak binding to the DNA under neutral to weakly basic conditions (pH 7.4, 8.2). However, no binding occurred at the lower pH of 5.0 and 6.0. As a control, Zn^{2+}-containing insulin failed to bind to DNA regardless of the pH. This result indicates that the binding of this poly-C DNA was not due to the formation of the i-motif. Instead, the formation of the i-motif inhibited binding. We previously observed that C-rich DNA adsorbed strongly to various nanomaterials, where low pH also weakened the adsorption.[37-39] The explanation was the lack of stable secondary structures for C-rich DNA at high pH, so that more cytosine bases can interact with surfaces or insulin.

Poly-C DNA as a General Protein Binder.

Because poly-C DNA exhibited a strong tendency to bind Zn^{2+}-free insulin, it might be a better aptamer candidate compared to poly-G DNA. To qualify to be an aptamer, specificity needs to be demonstrated. We then evaluated the binding of FAM-C30 to three proteins: BSA, human albumin, and hemoglobin. By measuring the increase in the FP signal in this system in response to each protein, we found that all of these proteins could trigger a remarkable signal increase (Figure 6B,

blue bars). We then gradually titrated each protein and calculated their K_d values (Figure 6C). Both BSA and human albumin had K_d values just below 1 μM, although hemoglobin showed weaker binding with a K_d of 18 μM. Interestingly, none of these proteins showed a sigmoidal binding curve, indicating that each aptamer binds to one protein. Compared to typical protein binding aptamers with K_d in the low nM range, this FAM-C30 DNA has much higher K_d values. Nevertheless, it indicates the general protein binding ability of poly-C DNA. Consequently, Poly-C DNA could not be used as an aptamer for the detection of insulin.

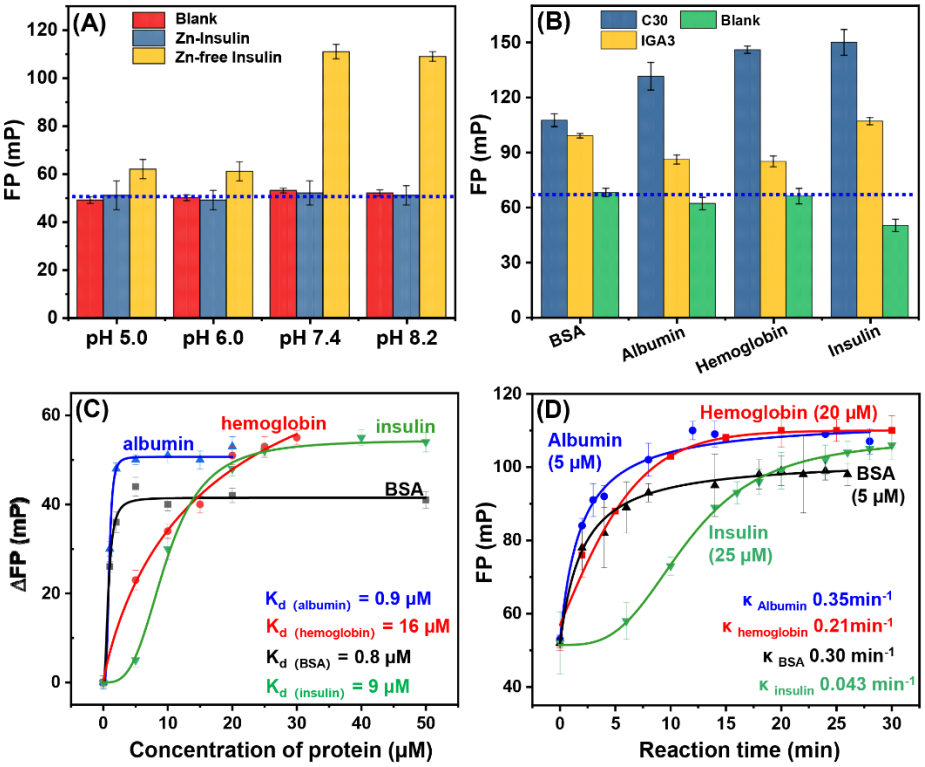


Figure 6. (A) FP assay of 40 nM Cy3-laabeled C15 DNA binding to insulin under different pH conditions. The error bars show the standard deviation from three replicates. (B) FP of 100 nM FAM-C30 DNA and FAM-IGA3 in the presence of BSA (50 μM), albumin (50 μM) hemoglobin (50 μM), and insulin (25 μM). (C) The FP assay of 100 nM FAM-C30 binding to different proteins at different concentrations. (D) Kinetics of 100 nM FAM-C30 binding to different proteins (5 μM BSA, 5 μM albumin, 20 μM hemoglobin, 25 μM insulin).

We also tested the binding of FAM-IGA3 to these proteins and they also resulted in a high FP signal (Figure 6B, yellow bars). This suggests that IGA3 does not specifically recognize insulin either. In the original aptamer selection paper, selectivity was characterized by the clotting time

by fusing the insulin aptamer to a thrombin aptamer, and the difference between insulin and BSA was quite small either.[15] We further tested the kinetics of FAM-C30 DNA to four proteins: BSA, human albumin, hemoglobin, and insulin (Figure 6D). BSA, albumin, and hemoglobin showed a normal pseudo first-order reaction profile. This is in contrast to the insulin data with an induction period, indicating that insulin binding was accompanied and facilitated by aggregation of multiple insulin molecules.

Further Discussion

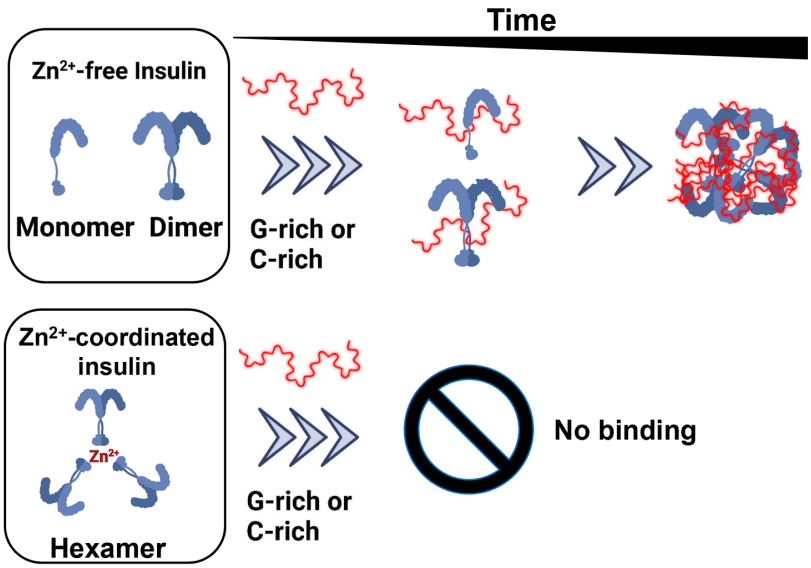
1. Insulin as a sensing target. Insulin hexamers are produced by the β-cells, and once released to blood, the concentration of insulin is drastically decreased, dissociating insulin to the monomers.[40] In the blood, monomeric insulin is the biologically active form, whereas hexametric insulin is the storage form. Although the detection of both monomers and hexamers is important, monomers are probably more important as a target. We searched the literature on the use of aptamers to detect insulin (Table S2), but most studies did not specify the method of insulin sample preparation. Considering the instability of insulin monomers in the buffer, EDTA-treated insulin could be a reasonable sample for analysis. The vendor of our insulin sample suggested acid treatment followed by neutralization, which should produce mainly hexamers that did not bind to our tested DNAs. For future biosensor studies, it is critical to fully describe the source of insulin and sample preparation method.

2. The IGA3 aptamer. While IGA3 DNA can be called an aptamer for insulin since it was obtained from in vitro selection using insulin as a target,[15] we obtained better binding sequences in this study. However, the binding of insulin by poly-C DNA is nonspecific, since other proteins (and various material surfaces) can also bind to poly-C DNA with even better affinities.[41] Therefore, it was impossible to use this DNA for the specific detection of insulin. New aptamer selection needs to be performed for this purpose. Nevertheless, poly-C DNA provides a benchmark for comparison with future aptamers, and aptamers should be able to bind better than poly-C DNA.

3. Nonspecific binding of DNA oligonucleotides to proteins has been documented, mainly for G-rich DNA. The G-quadruplex can bind to proteins, and the common types of binding are top-stacking, groove-binding, and loop-binding.[42] For example: tyr142 in telomeric proteins reaches into the G-quadruplex groove and interacts with several guanosines; and the His153 and Thr156 in zinc finger proteins (ZFP) bind to the loop phosphate backbone of G-quadruplex DNA.[43-44]

Many protein binding aptamers have a G-quadruplex structure, and the most famous is the thrombin-binding aptamer.[45] In contrast, little is known regarding about the binding of poly-C DNA to proteins. A classic case of a poly-C-binding protein is the specific binding of the KH3 domain in heterogeneous nuclear ribonucleoprotein (hnRNP) K to the TCCC and CCCC sequences.[46-49] In this work, we showed that poly-C or C-rich DNA can bind to various proteins. For most aptamers, binding occurred immediately after mixing with target proteins. For insulin, due to its unique aggregation property, characterization of its binding kinetics is especially important.

4. As a summary of understanding, our results showed that insulin in high aggregation state (hexamers, fibrils) hardly interacted with the IGA3 aptamer or poly-C DNA, while the FP signal was enhanced after mixing insulin with the IGA3 aptamer and poly-C DNA in low aggregation state (oligomers, dimers and monomer) (Scheme 1).



Scheme 1. Schematic illustrating the binding of insulin of different aggregation states to G-rich and C-rich DNA strands. For Zn^{2+}-free insulin, there is a time-dependent aggregation process, whereas the Zn^{2+}-coordinated insulin hexamers do not bind to these DNA sequences.

CONCLUSIONS

In this work, we prepared insulin solutions using various methods and studied their binding to various DNA sequences. Binding was observed only in insulin samples treated with a high concentration of EDTA, which sequestered Zn^{2+} from insulin, leading to the formation of monomers and dimers. These unstable insulin molecules then aggregated around the negatively charged DNA sequences, with the most favorable binding observed with C-rich DNA. The previously reported guanine-rich aptamer showed slower binding, and binding was observed only when 20 μM or more insulin was present. Poly-A and poly-T DNA did not show any binding under any of the tested conditions. Overall, C-rich DNAs are a better insulin binder in terms of both binding affinity and kinetics. However, C-rich DNAs are nonspecific and also bind to other proteins such as BSA. In addition, for future biosensor work for the detection of insulin, it is critical to clearly specify the method of sample preparation. These results provide further insight into the mechanism that control the binding between oligomeric insulin and DNA, which will be useful for the selection of new insulin binding aptamers and development of related biosensors.

CONFLICTS OF INTEREST

There are no conflicts to declare.

ASSOCIATED CONTENT

SUPPORTING INFORMATION

Table S1-S2: Sequences of the oligonucleotides used in this work; the treatment of insulin (hexamer). Figure S1-S7: Insulin (with Zn^{2+} and Zn^{2+}-free) mixed with ThT; TEM images of insulin (Zn^{2+} and Zn^{2+}-free); standard curve of Zn^{2+}; the effect of free fluorescein binding to insulin; the effect of EDTA; the effect of ionic strength for insulin binding to aptamer; the effect of incubation time of EDTA-insulin (Zn^{2+} and Zn^{2+}-free) then binding to the IGA3 aptamer (PDF)

AUTHOR INFORMATION

Juewen Liu - Department of Chemistry, Waterloo Institute for Nanotechnology, University of Waterloo, Waterloo, Ontario N2L 3G1, Canada.

orcid.org/0000- 0001-5918-9336; Email: liujw@uwaterloo.ca

Author

Na Wu- Research Center for Analytical Sciences, Department of Chemistry, College of Sciences, Northeastern University, Box 332, Shenyang 110819, China; Department of Chemistry, Waterloo Institute for Nanotechnology, University of Waterloo, Waterloo, Ontario N2L 3G1, Canada.

Mohamad Zandieh - Department of Chemistry, Waterloo Institute for Nanotechnology, University of Waterloo, Waterloo, Ontario N2L 3G1, Canada.

Ting Yang- Research Center for Analytical Sciences, Department of Chemistry, College of Sciences, Northeastern University, Box 332, Shenyang 110819, China.

ACKNOWLEDGMENTS

Funding for this work was from the Natural Sciences and Engineering Research Council of Canada (NSERC). Na Wu was supported by a China Scholarship Council (CSC) scholarship to visit the University of Waterloo.

REFERENCES

1. Sen, S.; Ali, R.; Onkar, A.; Ganesh, S.; Verma, S. Strategies for Interference of Insulin Fibrillogenic: Challenges and Advances. *ChemBioChem*. **2022***, 23, 11,* e202100678.
2. Mayer, J. P.; Zhang, F. Z.; Richard, D.; Marchi, D. Insulin Structure and Function. *Biopolymers*. **2007***, 5, 88,* 687-713.
3. Nielsen, L.; Khurana, R.; Coats, A.; Frokjaer, S.; Brange, J.; Vyas, S.; Uversky, V. N.; Fink, A. L. Effect of Environmental Factors on the Kinetics of Insulin Fibril Formation: Elucidation of the Molecular Mechanism. *Biochemistry*. **2001***, 40,* 6036-6046.
4. Nielsen, L.; Frokjaer, S.; Brange, J.; Vladimir, N.; Fink, A. L. Probing the Mechanism of Insulin Fibril Formation with Insulin Mutants. *Biochemistry*. **2001***, 40,* 28, 8397-8409.
5. Alijanvand, S. H.; Christensen, M.H.; Christiansen, G.; Harikandei, K. B.; Salehi, P.; Schiott, B.; Movahedi, A. A.; Otzen, D. E. Novel Noscapine Derivatives Stabilize the Native State of Insulin Against Fibrillation. *Int. J. Biol. Macromol*. **2020***, 147,* 98-108.
6. Malik, R.; Roy, I. Probing the Mechanism of Insulin Aggregation During Agitation. *Int. J. Pharmaceut.* **2011***, 413,* 1, 73-80.

7. Nuhu, M. M.; Curtis, R. Arginine Dipeptides Affect Insulin Aggregation in A pH- and Ionic Strength-Dependent Manner. *Biotechnol. J.* **2015***, 10, 3,* 404-416.

8. Pounot, K.; Grime, G. W.; Longo, A.; Zamponi, M.; Noferini, D.; Cristiglio, V.; Seydel, T.; Garman, E. F.; Weik, M.; Fodera, V.; Schiro, G. Zinc Determines Dynamical Properties and Aggregation Kinetics of Human Insulin. *Biophys. J.* **2021***, 120,* 5, 886-898.

9. Xu, Y. S.; Yan, Y. F.; Seeman, D.; Sun, L. H.; Dubin, P. L. Multimerization and Aggregation of Native-State Insulin: Effect of Zinc. *Langmuir*. **2012***, 28,* 579-586.

10. Ludwig, D. B.; Webb, J. N.; Fernandez, C.; Carpenter, J. F.; Randolph, T. W. Quaternary Conformational Stability: The Effect of Reversible Self-association on the Fibrillation of Two Insulin Analogs. *Biotechnol. Bioeng*. **2011***, 108,* 10, 2359-2370.

11. Catasti, P.; Chen, X.; Robert, K.; Moyzis, E.; Bradbury, M.; Gupta, G. Structure-Function Correlations of the Insulin-Linked Polymorphic Region. *J. Mol. Biol*. **1996***, 264,* 534-545.

12. Paritala, H.; Firestine, S. M. Characterization of Insulin ILPR Sequences for Their Ability to Adopt a G-Quadruplex Structure. *Nucleos. Nucleot. Nucl*.**2010***, 29, 2,* 81-90.

13. Schonhoft, J. D.; Das, A.; Achamyeleh, F.; Samdani, S.; Sewell, A.; Mao, H. B.; Basu, S. ILPR Repeats Adopt Diverse G-Quadruplex Conformations that Determine Insulin Binding. *Biopolymers*. **2010***, 93,* 1, 21-31.

14. Connor, A. C.; Frederick, K. A.; Morgan, E. J.; McGown, L. B. Insulin Capture by an Insulin-Linked Polymorphic Region G-Quadruplex DNA Oligonucleotide. *J. Am. Chem. Soc.* **2006***, 128,* 4986-4991.

15. Yoshida, W.; Mochizuki, E.; Takase, M.; Hasegawa, H.; Morita, Y.; Yamazaki, H.; Sode, K.; Ikebukuro, K. Selection of DNA Aptamers Against Insulin and Construction of an Aptameric Enzyme Subunit for Insulin Sensing. *Biosens. Bioelectron*. **2009***, 5, 24,* 1116-1120.

16. Habibi, E.; Omidinia, E.; Heidari, H.; Fazli, M. Flow Injection Amperometric Detection of Insulin at Cobalt Hydroxide Nanoparticles Modified Carbon Ceramic Electrode. *Anal. Biochem*. **2016***, 495,* 37-41.

17. Yoshida, W.; Mochizuki, E.; Takase, M.; Hasegawa, H.; Morita, Y.; Yamazaki, H.; Sode, K.; Ikebukuro, K. Selection of DNA Aptamers Against Insulin and Construction of an Aptameric Enzyme Subunit for Insulin Sensing. *Biosens. Bioelectron*. **2009***, 5, 24,* 1116-1120.

18. Sahin, S.; Kaya, S.; Ustundag, Z.; Caglayan, M. O. An Electrochemical Signal Switch-Based (On-Off) Aptasensor for Sensitive Detection of Insulin on Gold-Deposited Screen-Printed Electrodes. *J. Solid State Electronics* **2022***, 26, 4,* 907-915.

19. Taib, M.; Tan, L. L.; Abd Karim, N. H.; Ta, G. C.; Heng, L. Y.; Khalid, B. Reflectance Aptasensor Based on Metal Salphen Label for Rapid and Facile Determination of Insulin. *Talanta* **2019***, 207,* 120321.

20. Wu, Y.; Midinov, B.; White, R. J. Electrochemical Aptamer-Based Sensor for Real-Time Monitoring of Insulin. *ACS Sensors* **2019***, 4, 2,* 498-503.

21. Torosantucci, R.; Kukrer, B.; Mero, A.; Van Winsen, M.; Tantipolphan, R.; Jiskoot, W. Plain and Mono-Pegylated Recombinant Human Insulin Exhibit Similar Stress-Induced Aggregation Profiles. *J. Pharm. Sci*. **2011***, 100, 7,* 2574-2583.

22. Wasko, J.; Wolszczak, M.; Kaminski, Z. J.; Steblecka, M.; Kolesinska, B. Human Serum Albumin Binds Native Insulin and Aggregable Insulin Fragments and Inhibits Their Aggregation. *Biomolecules*. **2020***, 10, 10,* 1366.

23. Gong, H.; He, Z. H.; Peng, A. L.; Zhang, X.; Cheng, B. A.; Sun, Y.; Zheng, L.; Huang, K. Effects of Several Quinones on Insulin Aggregation. *Sci. Rep*. **2014***, 4,* 5648.

24. Pounot, K.; Grime, G. W.; Longo, A.; Zamponi, M.; Noferini, D.; Cristiglio, V.; Seydel, T.; Garman, E. F.; Weik, M.; Fodera, V. Zinc Determines Dynamical Properties and Aggregation Kinetics of Human Insulin. *Biophys. J*. **2021***, 120, 5,* 886-898.

25. Coffman, F. D.; Dunn, M. F. Insulin-Metal Ion Interactions: The Binding of Divalent Cations to Insulin Hexamers and Tetramers and the Assembly of Insulin Hexamers. *Biochemistry*. **1988***, 27,* 6179-6187

26. Taghdisi, S. M.; Danesh, N. M.; Lavaee, P.; Emrani, A. S.; Ramezani, M.; Abnous, K. Aptamer Biosensor for Selective and Rapid Determination of Insulin. *Anal. Lett*. **2015***, 48, 4,* 672-681.

27. Bentea, L.; Watzky, M. A.; Finke, R.G. Sigmoidal Nucleation and Growth Curves Across Nature Fit by the Finke-Watzky Model of Slow Continuous Nucleation and Autocatalytic Growth: Explicit Formulas for the Lag and Growth Times Plus Other Key Insights. *J. Phys. Chem. C.* **2017***, 121,* 5302-5312.

28. Librizzi, F.; Rischel, C. The Kinetic Behavior of Insulin Fibrillation is Determined by Heterogeneous Nucleation Pathways. *Protein Sci*. **2005***, 14, 12,* 3129-3134.

29. Baram, M.; Gilead, S.; Gazit, E.; Miller, Y. Mechanistic Perspective and Functional Activity of Insulin in Amylin Aggregation. *Chem Sci*. **2018***, 9, 18,* 4244-4252.

30. Manno, M.; Craparo, E. F.; Martorana, V.; Bulone, D.; San, Biagio. P. L. Kinetics of Insulin Aggregation: Disentanglement of Amyloid Fibrillation from Large-Size Cluster Formation. *Biophys. J*. **2006***, 90, 12,* 4585-4591.

31. Doghaeaei, A.V.; Housaindokht, M. R.; Spectroscopic Study of the Interaction of Insulin and Its Aptamer-Sensitive Optical Detection of Insulin. *J. Lumin*. **2015***, 159,* 1-8.

32. Ziaunys, M.; Sakalauskas, A.; Mikalauskaite, K.; Smirnovas, V. Exploring the Occurrence of Thioflavin-T-Positive Insulin Amyloid Aggregation Intermediates. *PeerJ* **2021***, 9,* e10918.

33. Sulatsky, M. I.; Sulatskaya, A. I.; Pova rova, O. I.; Antifeeva, I. A.; Kuznetsova, I. M.; Turoverov, K. K. Effect of the Fluorescent Probes ThT and ANS on the Mature Amyloid Fibrils. *Prion*. **2020***, 14,* 67-75.

34. Verdian-Doghaei, A.; Housaindokht, M. R.; Bozorgmehr, M. R.; Abnous, K. Conformational Switch of Insulin-Binding Aptamer into G-Quadruplex Induced by K^+ and Na^+: An Experimental and Theoretical Approach. *J. Biomol. Struct. Dyn*. **2015***, 33,*1153-1163.

35. Antolíková, E.; Žáková, L.; Turkenburg, J. P.; Watson, C. J.; Hančlová, I.; Šanda, M.; Cooper, A.; Kraus, T.; Brzozowski, A. M.; Jiráček J. Non-Equivalent Role of Inter-and Intramolecular Hydrogen Bonds in the Insulin Dimer Interface. *J. Biol. Chem*. **2011***, 286,* 36968-36977.

36. Coval, M.L. Analysis of Hill Interaction Coefficients and the Invalidity of the Kwon and Brown Equation. *J. Biol. Chem*. **1970***, 245,* 6335-6336.

37. Lopez, A.; Zhao, Y.; Huang, Z. C.; Guo, Y. F.; Guan, S. K.; Jia, Y.; Liu, J. W. Poly-Cytosine Deoxyribonucleic Acid Strongly Anchoring on Graphene Oxide Due to Flexible Backbone Phosphate Interactions. *Adv. Mater. Interfaces* **2021***, 8,* 2001798.

38. Wang, Z.; Huang, Z. C.; Han, J.; Xie, G.; Liu, J. W. Polyvalent Metal Ion Promoted Adsorption of DNA oligonucleotides by Montmorillonite. *Langmuir*. **2021***, 37,* 1037-1044.

39. Chang, Y. Y.; Liu, B. W.; Huang, Z. C.; Liu, Y. B.; Liu, M.; Liu, J. W. Yttrium Oxide as a Strongly Adsorbing but Non-Quenching Surface for DNA Oligonucleotides. *Langmuir*. **2020***, 36,* 1034-1042.

40. Fu, Z.; Gilbert, E. R.; Liu, D. Regulation of Insulin Synthesis and Secretion and Pancreatic Beta-Cell Dysfunction in Diabetes. *Curr. Diabetes Rev*. **2013***, 9,* 25-53.

41. Lu, C.; Huang, Z. C.; Liu, B. W.; Liu, Y. B.; Ying, Y. B.; Liu, J. W. Poly-Cytosine DNA as a High-Affinity Ligand for Inorganic Nanomaterials. *Angew. Chem. Int. Ed*. **2017***, 56,* 6208-6212.

42. Stephenson, V. M. G4-Quadruplex-Binding Proteins: Review and Insights into Selectivity. *Biophys. Rev*. **2022***, 14,* 635-654.

43. Shu, H. L.; Zhang, R. X.; Xiao, K.; Yang, J.; Sun, X. G-quadruplex-Binding Proteins: Promising Targets for Drug Design. *Biomolecules*. **2022***, 12,* 648.

44. Brázda, V.; Hároníková, L.; Jack, C.; Fojta, M. DNA and RNA Quadruplex-Binding Proteins. *Int. J. Mol. Sci*. **2014***, 15,* 17493-17517.

45. Macaya, R. F.; Schultze, P.; Smith, F. W.; Roe, J. A.; Feigon, J., Thrombin-Binding DNA Aptamer Forms a Unimolecular Quadruplex Structure in Solution. *Proc. Natl. Acad. Sci. U.S.A.* **1993**, 90, 3745-3749.

46. Makeyev, A. V.; Liebhaber, A. S. The Poly(C)-Binding Proteins: A Multiplicity of Functions and a Search for Mechanisms. *RNA*. **2002***, 8,* 265-278.

47. Kang, D.H.; Song, K.Y.; Wei, L. N.; Yee Law, P. Y.; Loh, H. H.; Choi, H. S. Novel Function of the Poly(C)-Binding Protein A-CP2 as a Transcriptional Activator that Binds to Single-Stranded DNA Sequences. *Int. J. Mol. Med.* **2013***, 32,* 1187-1194.

48. Backe, P. H.; Messias, A. C.; Ravelli, R.; Sattler, M.; Cusack, S. X-ray Crystallographic and NMR Studies of the Third KH Domain of hnRNP K in Complex with Single-Stranded Nucleic Acids. *Structure*. **2005***, 13,* 1055-1067.

49. Wu, W. Q.; Zhang, X.; Bai, D.; Shan, S. W.; Guo, L. J. Mechanistic Insights into Poly(C)-Binding Protein hnRNP K Resolving i-Motif DNA Secondary Structures. *J. Biol. Chem*. **2022***, 12,* 102670.

For Table of Contents Only

